



Pergamon

Available online at www.sciencedirect.com

SCIENCE @ DIRECT®

ENERGY

Energy 28 (2003) 539–556

www.elsevier.com/locate/energy

Energy and exergy analyses of solar drying process of pistachio

A. Midilli ^{a,*}, H. Kucuk ^b

^a *Mechanical Engineering Department, University of Nigde, Nigde 51000, Turkey*

^b *Mechanical Engineering Department, Karadeniz Technical University, Trabzon 61080, Turkey*

Received 20 April 2001

Abstract

This paper is concerned with the energy and exergy analyses of the drying process of shelled and unshelled pistachios using a solar drying cabinet. Using the first law of thermodynamics, energy analysis was carried to estimate the amounts of energy gained from solar air collectors and the ratios of energy utilization. However, exergy analysis was accomplished to determine the location, type, and magnitude of exergy losses during the solar drying process by applying the second law of thermodynamics. It was deduced that the exergy losses took place mostly in the 15th shelf where the available energy was less utilized. Moreover, the shelled and unshelled pistachios are sufficiently dried in the ranges between 40 and 60 °C and 37 and 62% of relative humidity at 1.23 m s⁻¹ of drying air velocity in 6 h despite the exergy losses of 0.15–3.08 kJ kg⁻¹.

© 2003 Elsevier Science Ltd. All rights reserved.

1. Introduction

Drying, used to preserve agricultural products, is a complex process involving heat and mass transfer between the product surface and its surrounding medium and within the product [1]. It can be conducted with a renewable energy source such as solar energy. In the solar drying process, the heat required is supplied from the sun [2]. To reduce the energy expenses during drying process, the farmers generally make use of solar energy.

Although many experimental and theoretical studies on the solar drying process exist in literature, there is limited study on the energy and exergy analyses of this process. As known, exergy analysis evaluates the available energy at different points in a system. In the design of a system,

* Corresponding author. Tel.: +90-388-2250115; fax: +90-388-2250112.

E-mail addresses: midilli@nigde.edu.tr (A. Midilli); hkucuk@ktu.edu.tr (H. Kucuk).

Nomenclature

Symbols

A	area, m^2
b	constant of drying velocity, h^{-1}
c_p	specific heat, $\text{kJ kg}^{-1} \text{K}^{-1}$
\bar{c}_p	mean specific heat, $\text{kJ kg}^{-1} \text{K}^{-1}$
E	emissive power
EUR	energy utilization ratio, %
Ex	exergy, kJ kg^{-1}
F	shape factor
g	gravitational acceleration, m s^{-2}
g_c	constant in Newton's law
h	enthalpy, kJ kg^{-1}
J	joule constant
\dot{m}	mass flow rate, kg s^{-1}
N	number of species
P	pressure, kPa
Q	net heat, kJ s^{-1}
Q_u	useful energy gained by solar air collector, kJ s^{-1}
s	specific entropy, $\text{kJ kg}^{-1} \text{K}^{-1}$
t	time, h
T	temperature, K
u	specific internal energy, kJ kg^{-1}
v	specific volume, $\text{m}^3 \text{kg}^{-1}$
V	velocity, m s^{-1}
w	specific humidity, g g^{-1}
W	moisture content, %
\dot{W}	energy utilization, J s^{-1}
z	altitude coordinate, m

Greek symbols

ϕ	relative humidity, %
η_{Ex}	exergetic efficiency, %
μ	chemical potential, kJ kg^{-1}
ρ	density, kg m^{-3}

subscripts

i	inlet, inflow
o	outlet
da	drying air
c	collector, chemical
dc	drying cabinet
f	fan
L	loss
mp	moisture of product
mz	mixed zone
o	outflow
sac	solar air collector
sat	saturated
sh2	the 2nd shelf
sh15	the 15th shelf
sp	shelled pistachio
up	unshelled pistachio
∞	surrounding or ambient

the exergy method provides the useful information to choose the appropriate component design and operation procedure. This information is much more effective in determining the plant and operation cost, energy conservation, fuel versatility and pollution. Bejan [3] pointed out that the minimization of lost work in the system would provide the most efficient system. Moreover, Bejan [4] and Szargut et al. [5] emphasized that the effect of operating conditions on the system efficiency was much stronger for lost-work analysis than it is for the heat balance analysis. This explanation is required to determine the inefficient process, equipment, or operating procedure during solar drying.

In this paper, energy and exergy analyses of solar drying process of shelled and unshelled pistachios were carried out. Consequently, it was found that the exergy losses took place mostly in the shelf 15 where the available energy was less utilized.

2. Material and procedure

2.1. Experimental set-up

The experimental set up, shown in Fig. 1, consists of a drying cabinet, solar air collector, and auxiliary heater and circulation fan. Drying cabinet is $55 \times 92 \times 117 \text{ cm}^3$ and has 16 shelves, which were made of wire-mesh-bottomed trays. The 4.5 m^2 solar air collector (collectors area = $2 \times (1.25 \times 1.8 \text{ m}^2)$) was connected to solar drying cabinet, and was used when

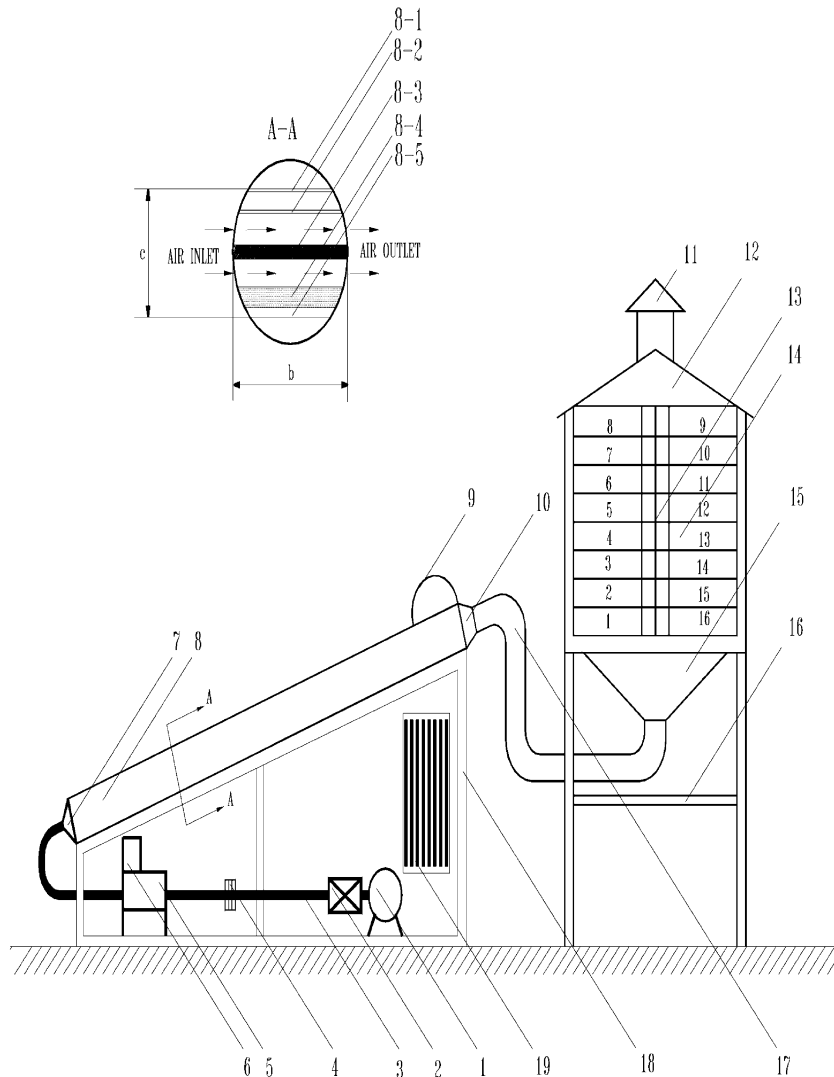


Fig. 1. Solar assisted drying cupboard (1. Fan, 2. Valve, 3. Connection pipe, 4. Orifice, 5. Auxiliary heater, 6. Temperature controller, 7. Inlet of solar air collectors, 8. Solar air collectors (2), 8-1. Glass cover, 8-2. Glass cover, 8-3. Absorber plate, 8-4. Insulation, 8-5. Wood cover, 9. Pyranometer, 10. Outlet of solar air collectors, 11. Chimney, 12. Outlet of drying cupboard, 13. Inter section, 14. Shelves, 15. Inlet of drying cupboard, 16. Support of drying cupboard, 17. Flexible connection pipe, 18. Support of solar air collector, 19. Manometer).

solar radiation was intense. The circulation fan to supply fresh air has a power of 0.37 kW and was connected to the inlet of the electric furnace.

2.2. Experimental procedure

Solar drying process was conducted using a solar drying cabinet in late summer 1999 in Trabzon, Turkey with a maximum and minimum air temperatures of around 32 and 21 °C, respectively,

relatively low air humidity that never exceed 75%, and under solar radiation varying between 200 and 808 W m⁻². Midilli [6] determined that, before drying experiments, the initial moisture contents of pistachio samples were 26.95% for shelled pistachio and 29.00% for unshelled pistachio.

In the experiments, the 2nd and 15th shelves were selected for the efficient utilization of drying air. However, the 1st and 16th shelves were kept empty so that hot air could be homogeneously diffused throughout the shelves inside of the solar drying cabinet. One hundred grams each of shelled and unshelled pistachio was placed as single layer of 9.8 and 7.8 mm thickness, respectively, on the 2nd and 15th shelves. The reason for the utilization of 100 each g of the samples is that the capacities of the shelves in the solar drying cabinet are enough to collect the required data from the experiments. In order to sufficiently dry the products, it is important to keep the drying air temperature constant. In solar drying processes, the drying air temperature can vary based on the magnitude of the solar radiation. In this study, the solar air collector heated the fresh air to 40–84 °C depending on daily ranges of the solar energy, which varied from 200 to 808 W m⁻². However, it was noticed that the temperatures of drying air decreased to 34–82 °C at the inlet of the shelves because of the heat loss throughout the connection pipe between the outlet of the solar air collector and the inlet of the solar drying cabinet.

Midilli [6] presented the detailed experimental procedure in literature. A small electronic balance (Mettler Pm 6100) was used to weigh the shelves. The amounts of solar radiation were measured with Kip-Zonen Solarymeter. All temperatures in solar drying cabinet were determined with Cr–Al thermocouples and the outlet temperatures were measured with thermometer. The dry-bulb and wet-bulb temperatures were gauged with Aspirated Hygrometer and the values of relative humidity were determined using Psychrometric Chart. Pressure drops at inlet–outlet of orifice, settled at the outlet of the fan, were measured with a water manometer to estimate the velocity of the drying air passing through the solar air collectors. Drying air velocity at the outlet of the circulation fan was estimated as 12.3 m s⁻¹ while wind velocity was determined as almost 0.8 m s⁻¹ by meteorological observations. However, drying air velocity throughout the shelves was approximately measured as 1.23 m s⁻¹ with an anemometer (TA2 air flow meter).

3. Analysis

Solar drying process was considered as a steady-flow process in these analyses.

3.1. The first law analysis: energy utilization

The air conditioning process throughout the solar drying of pistachios includes the processes of heating, cooling, and humidification. The air conditioning processes can be modeled as steady-flow processes that are analyzed by applying the steady-flow conservation of mass (for both dry air and moisture) and conservation of energy principles.

General equation of mass conservation of drying air:

$$\sum \dot{m}_{ai} = \sum \dot{m}_{ao} \quad (1)$$

General equation of mass conservation of moisture:

$$\sum(\dot{m}_{wi} + \dot{m}_{mp}) = \sum \dot{m}_{wo} \quad \text{or} \quad \sum(\dot{m}_{ai}w_i + \dot{m}_{mp}) = \sum \dot{m}_{ai}w_o \quad (2)$$

General equation of energy conservation:

$$\dot{Q} - \dot{W} = \sum \dot{m}_o \left(h_o + \frac{V_o^2}{2} \right) - \sum \dot{m}_i \left(h_i + \frac{V_i^2}{2} \right) \quad (3)$$

The changes in kinetic energy of the fan were taken into consideration while the potential and kinetic energy in other parts of the process were neglected. During the energy and exergy analyses of pistachio drying process, the following equations were generally used to compute the relative humidity and enthalpy of drying air.

The relative humidity

$$\phi = \frac{wP}{(0.622 + w)P_{\text{sat}@T}} \quad (4)$$

where w denotes the specific humidity, P the atmospheric pressure, and $P_{\text{sat}@T}$ is the saturated vapor pressure of drying air.

The enthalpy of drying air

$$h = c_{pda}T + wh_{\text{sat}@T} \quad (5)$$

where c_{pda} defines the specific heat of drying air, T the drying air temperature and $h_{\text{sat}@T}$ is the enthalpy of the saturated vapor.

3.1.1. Determination of the fan outlet conditions

The enthalpy equation of the fan outlet was derived [7] by using Eq. (1) as

$$h_{fo} = \left[\left(\dot{W}_f - \frac{V_{fo}^2}{2 \times 1000} \right) \left(\frac{1}{\dot{m}_{da}} \right) \right] + h_{fi} \quad (6)$$

where h_{fi} characterizes the enthalpy of drying air at the inlet of the fan, h_{fo} the enthalpy at the outlet of the fan, v_{fo} the drying air velocity at the outlet of the fan, fan energy and \dot{m}_{da} is the mass flow of drying air.

Considering the values of dry-bulb temperature and enthalpy from Eq. (6), the specific and relative humidity of drying air at the outlet of the fan were determined by using the Psychrometric Chart.

3.1.2. Determination of the outlet conditions of solar air collector

The inlet conditions of the solar air collectors were assumed as equal to the outlet conditions of the fan.

$$w_{ci} = w_{fo}T_{ci} = T_{fo}\phi_{ci} = \phi_{fo}h_{ci} = h_{fo} \quad (7)$$

In Eq. (7), subscript ci describes the solar air collector inlet and fo the fan outlet. The useful energy gained from the collectors was calculated using the magnitudes of the solar radiation by the following equation.

$$\dot{Q}_u = \dot{m}_{da} c_{pda} (T_{co} - T_{ci}) \quad (8)$$

The relative humidity (ϕ_{co}) and enthalpy (h_{co}) at the outlet of the solar air collectors were, respectively, found using Eqs. (4) and (5).

3.1.3. Determination of the outlet conditions of the 2nd and 15th shelves

The inlet conditions of the solar drying cabinet were determined depending on the inlet temperatures and specific humidity of drying air. The inlet conditions of these shelves were assumed as equal to the inlet conditions of the solar drying cabinet. Meanwhile, it was considered that the mass flow rate of drying air was equal throughout the shelves (Fig. 2). This consideration can be justified as follows.

Total mass flow rate of drying air,

$$\dot{m}_{dci} = \dot{m}_{sh2} + \dot{m}_{sh15} \quad (9)$$

$$\rho_{da} A_{dci} V_{dci} = \rho_{da} A_{sh2} V_{sh2} + \rho_{da} A_{sh15} V_{sh15} \quad (10)$$

In Eq. (10),

$$V_{da} = V_{sh2} = V_{sh15} \quad \text{and} \quad A_{sh2} = A_{sh15} = 0.5 A_{dci} \quad (11)$$

Using Eqs. (9)–(11),

$$\dot{m}_{sh2} = \dot{m}_{sh15} = 0.5 \dot{m}_{dci} \quad (12)$$

Thus, the inlet conditions of the shelves can be written as follows.

For the 2nd and 15th shelves:

$$w_{dci} = w_{sh2i} = w_{sh15i} T_{dci} = T_{sh2i} = T_{sh15i} \phi_{dci} = \phi_{sh2i} = \phi_{sh15i} h_{dci} = h_{sh2i} \quad (13)$$

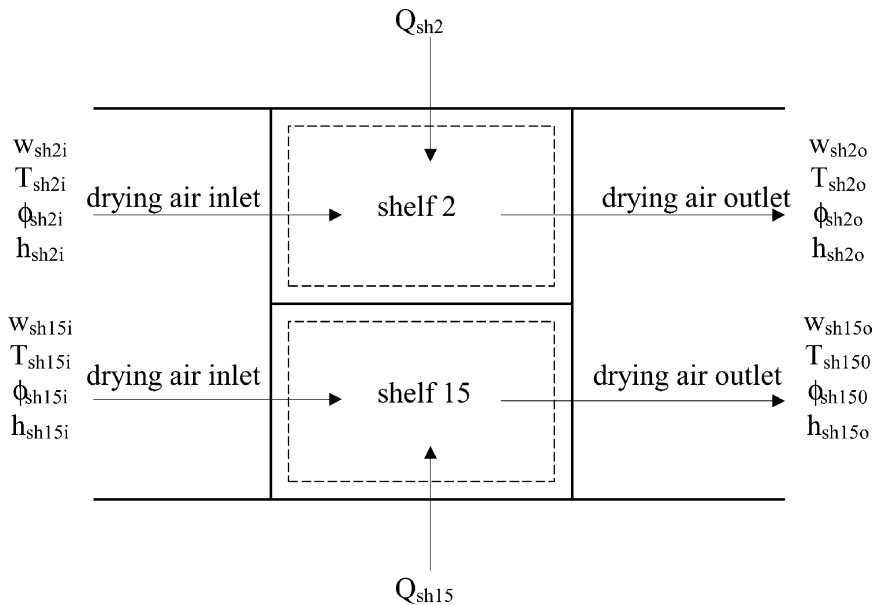


Fig. 2. Schematic illustration of the shelves.

$$= h_{sh15i} \dot{m}_{da,sh2i} = \dot{m}_{da,sh15i} = \dot{m}_{da}/2$$

Using Eqs. (1) and (2), the equations of the specific humidity at the outlet of the shelves were derived as follows.

For the 2nd shelf:

$$w_{sh2o} = w_{sh2i} + \frac{2\dot{m}_{wsp}}{\dot{m}_{da}} \quad (14)$$

For the 15th shelf:

$$w_{sh15o} = w_{sh15i} + \frac{2\dot{m}_{wup}}{\dot{m}_{da}} \quad (15)$$

Where, w_{sh2i} denotes the specific humidity at the inlet of the 2nd shelf, w_{sh15i} the specific humidity at the inlet of the 15th shelf, \dot{m}_{wsp} the mass flow rate of the moisture removed from shelled pistachio, \dot{m}_{wup} the mass flow rate of the moisture removed from unshelled pistachio.

The relative humidity and enthalpy of drying air at the outlet of the shelves were, respectively, estimated using Eqs. (4) and (5). During the humidification process at the shelves, the heat used was calculated by using the following equations.

For the 2nd shelf:

$$\dot{Q}_{sh2} = \frac{\dot{m}_{da}}{2} (h_{sh2i@T} - h_{sh2o@T}) \quad (16)$$

For the 15th shelf:

$$\dot{Q}_{sh15} = \frac{\dot{m}_{da}}{2} (h_{sh15i@T} - h_{sh15o@T}) \quad (17)$$

where, $h_{sh2i@T}$, $h_{sh2o@T}$, $h_{sh15i@T}$ and $h_{sh15o@T}$ identify orderly the enthalpies at the inlet and outlet of the 2nd and 15th shelves.

3.1.4. Determination of the outlet conditions of drying cabinet

The specific humidity at the outlet of the solar drying cabinet was determined as

$$w_{dco} = \frac{w_{sh2o} \dot{m}_{sh2o} + w_{sh15o} \dot{m}_{sh15o}}{\dot{m}_{sh2o} + \dot{m}_{sh15o}} \quad (18)$$

The values of the relative humidity and enthalpy at the outlet of the cabinet were calculated applying Eqs. (4) and (5).

During the solar drying process, the energy utilization ratios (EURs) of the shelves and cabinet were obtained.

For the 2nd shelf:

$$\text{EUR}_{\text{sh2}} = \frac{\dot{m}_{\text{sh2i}}(h_{\text{sh2i}@T} - h_{\text{sh2o}@T})}{\dot{m}_{\text{da}}c_{p\text{da}}(T_{\text{co}} - T_{\text{ci}})} \quad (19)$$

For the 15th shelf:

$$\text{EUR}_{\text{sh15}} = \frac{\dot{m}_{\text{sh15i}}(h_{\text{sh15i}@T} - h_{\text{sh15o}@T})}{\dot{m}_{\text{da}}c_{p\text{da}}(T_{\text{co}} - T_{\text{ci}})} \quad (20)$$

For the solar drying cabinet:

$$\text{EUR}_{\text{dc}} = \frac{\dot{m}_{\text{da}}(h_{\text{dci}@T} - h_{\text{dco}@T})}{\dot{m}_{\text{da}}c_{p\text{da}}(T_{\text{co}} - T_{\text{ci}})} \quad (21)$$

3.2. The second law analysis: exergy analysis

In the scope of the second law analysis of thermodynamics, total exergy inflow, outflow and losses of the shelves and the solar drying cabinet were estimated. The basic procedure for exergy analysis of the cabinet is to determine the exergy values at steady-state points and the reason of exergy variation for the process [4]. The exergy values are calculated by using the characteristics of the working medium from a first law energy balance [5]. For this purpose, the following equation [8] was employed.

$$\begin{aligned} \text{Exergy} = & \underbrace{(u - u_{\infty})}_{\text{internal energy}} - \underbrace{T_{\infty}(s - s_{\infty})}_{\text{entropy}} + \underbrace{\frac{P_{\infty}}{J}(v - v_{\infty})}_{\text{work}} + \underbrace{\frac{V^2}{2gJ}}_{\text{momentum}} + \underbrace{(z - z_{\infty})\frac{g}{g_cJ}}_{\text{gravity}} \\ & + \sum_c (\mu_c - \mu_{\infty})N_c + \underbrace{E_i A_i F_i (3T^4 - T_{\infty}^4 - 4T_{\infty}T^3)}_{\text{radiation emission}} + \dots \end{aligned} \quad (22)$$

where the subscript ∞ denotes the reference conditions.

There are variations of this general exergy equation. In the analyses of many systems, some, but not all, of the terms shown in Eq. (22) are used. Since exergy is energy available from any source, the terms can be developed using electrical current flow, magnetic fields, and diffusional flow of materials. One common simplification is to substitute enthalpy for the internal energy and Pv terms that are applicable for steady-flow systems. Eq. (22) is often used under conditions where the gravitational and momentum terms are neglected. In addition to these, the pressure changes in the system are also neglected because of $v \cong v_{\infty}$. In this case, Eq. (22) is derived as

$$\text{Exergy} = \bar{c}_p \left[(T - T_{\infty}) - T_{\infty} \ln \frac{T}{T_{\infty}} \right] \quad (23)$$

Applying Eq. (23), the inflow, and outflow of exergy can be found depending on the inlet and outlet temperatures of the shelves and the solar drying cabinet. Hence, the exergy loss is determined by Eq. (24).

$$\text{Exergy loss} = \text{Exergy inflow} - \text{Exergy outflow} \sum \text{Ex}_L = \sum \text{Ex}_i - \sum \text{Ex}_o \quad (24)$$

The equation of exergy inflow can be written for the shelves and the cabinet as

$$\text{Ex}_{\text{sh2i}} = \text{Ex}_{\text{sh15i}} = \text{Ex}_{\text{dci}} = \text{Ex}_{\text{shi}} = \bar{c}_{p_{\text{da}}} \left[(T_{\text{shi}} - T_{\infty}) - T_{\infty} \ln \frac{T_{\text{shi}}}{T_{\infty}} \right] \quad (25)$$

where $\bar{c}_{p_{\text{da}}}$ defines the average specific heat of drying air.

The equation of exergy outflow can be also written as follows.

For the 2nd shelf:

$$\text{Ex}_{\text{sh2o}} = \bar{c}_{p_{\text{da}}} \left[(T_{\text{sh2o}} - T_{\infty}) - T_{\infty} \ln \frac{T_{\text{sh2o}}}{T_{\infty}} \right] \quad (26)$$

For the 15th shelf:

$$\text{Ex}_{\text{sh15o}} = \bar{c}_{p_{\text{da}}} \left[(T_{\text{sh15o}} - T_{\infty}) - T_{\infty} \ln \frac{T_{\text{sh15o}}}{T_{\infty}} \right] \quad (27)$$

For the solar drying cabinet:

$$\text{Ex}_{\text{dco}} = \bar{c}_{p_{\text{da}}} \left[(T_{\text{dco}} - T_{\infty}) - T_{\infty} \ln \frac{T_{\text{dco}}}{T_{\infty}} \right] \quad (28)$$

Moreover, the quantity of the exergy losses is calculated by applying Eq. (24) to Eqs. (25)–(28). Because of this calculation procedure, the band diagram of exergy balance is shown in Fig. 3.

The exergetic efficiency can be defined as the ratio of the product exergy (exergy loss of each shelf) to exergy inflow for the shelves. However, it is explained as the ratio of exergy outflow to exergy inflow for the cabinet. Thus, the general form of exergetic efficiency is written as [9]

$$\text{Exergetic Efficiency} = \frac{\text{Exergy inflow} - \text{Exergy loss}}{\text{Exergy inflow}} \eta_{\text{Ex}} = 1 - \frac{\text{Ex}_L}{\text{Ex}_i} \quad (29)$$

4. Results and discussion

The required data were obtained using the derived equations for the energy and exergy analyses, and presented in Figs. 4–12 and Tables 1 and 2.

Fig. 4 indicates the variation of temperatures as a function of the solar radiation. It was observed that the temperatures of drying air varied between 40 and 84 °C depending on the ranges in solar energy, which varied from 200 to 808 W m⁻². In addition, its outlet temperature increased linearly with the rise in the magnitude of the solar radiation. However, the temperatures of drying air recorded at the inlet of the solar drying cabinet were between 34 and 82 °C while the outlet temperatures were between 34 and 56.4 °C. Moreover, the measured temperatures of the 2nd shelf were between 41 and 60 °C while those of the 15th shelf were between 40 and 55 °C. Accordingly, it is said that all temperatures of drying cabinet changed depending on the solar radiation, and were enough to begin and complete the drying experiments.

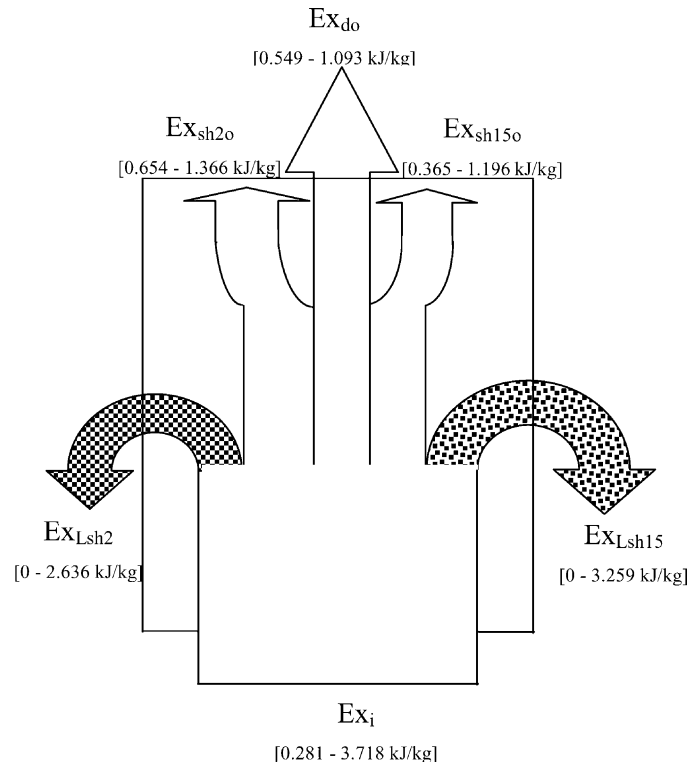


Fig. 3. Band diagram of exergy balance.

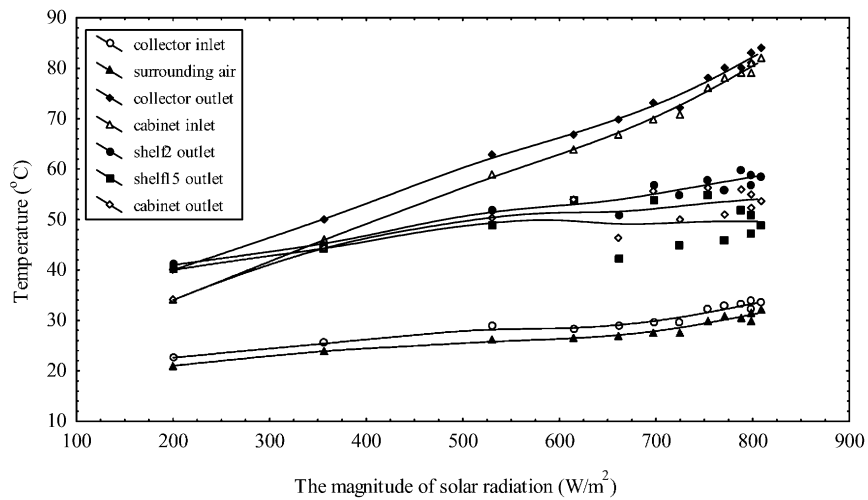


Fig. 4. Variation of temperatures in solar drying cabinet as a function of the magnitude of solar radiation.

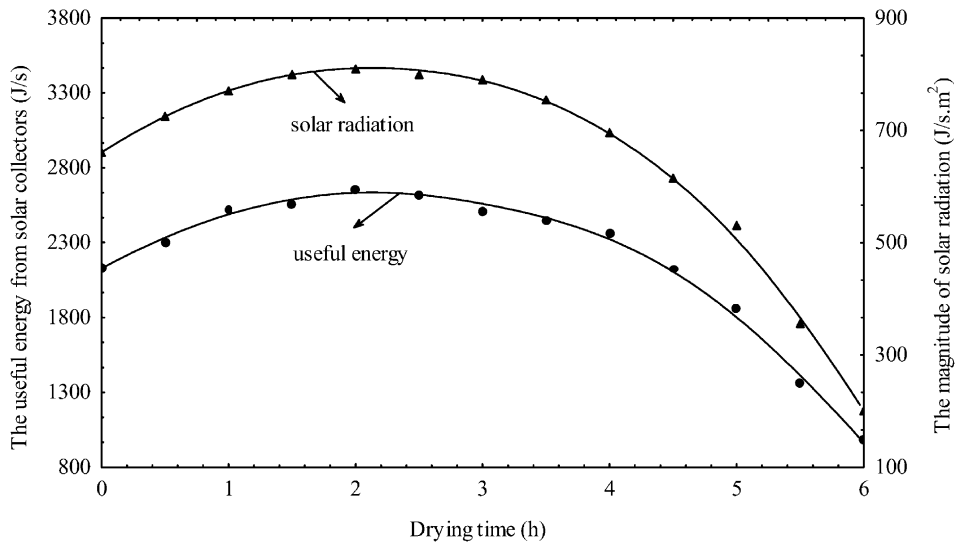


Fig. 5. Variation of useful energy from solar air collectors on the left ordinate and the magnitude of solar radiation on the right ordinate as a function of drying time.

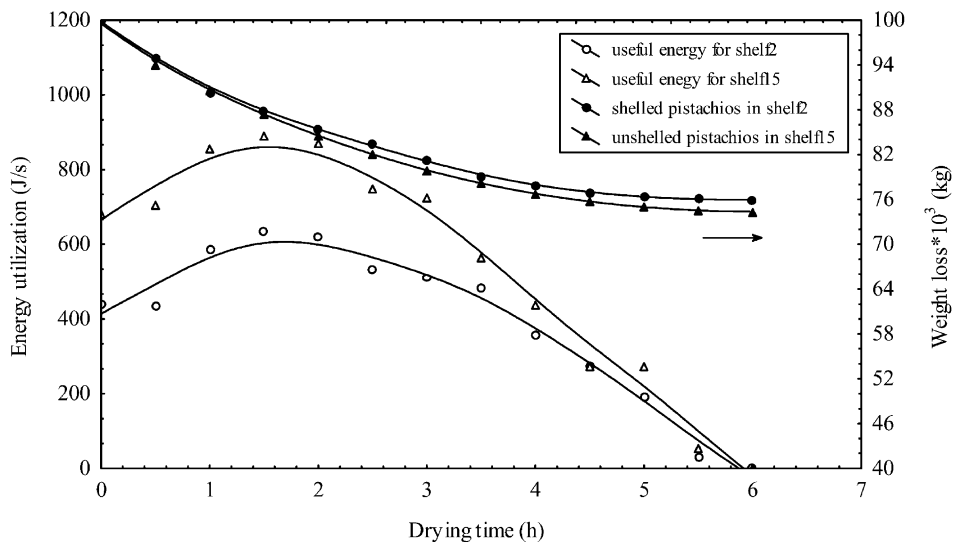


Fig. 6. The variations of energy utilization on the left ordinate and weight loss on the right ordinate as a function of drying time.

Fig. 5 shows the variation of the useful energy from the solar air collectors on the left ordinate and the magnitude of the solar radiation on the right as a function of drying time. The amounts of the useful energy from the solar air collectors were calculated using Eq. (8) based on the inlet and outlet temperatures of the collectors. It was observed that they varied between 977 and 2664 J s⁻¹ depending on the magnitude of the solar radiation. Consequently, it was found that the

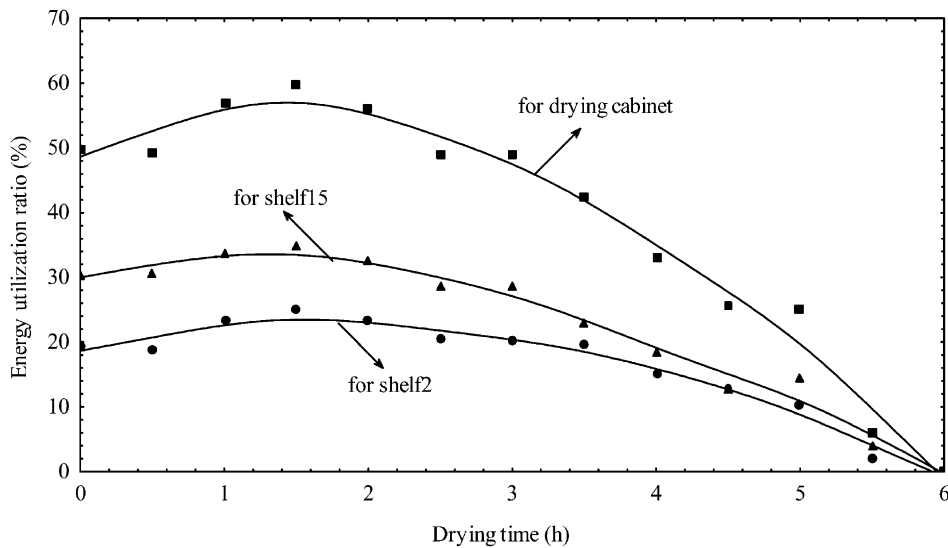


Fig. 7. Variation of EUR as a function of drying time.

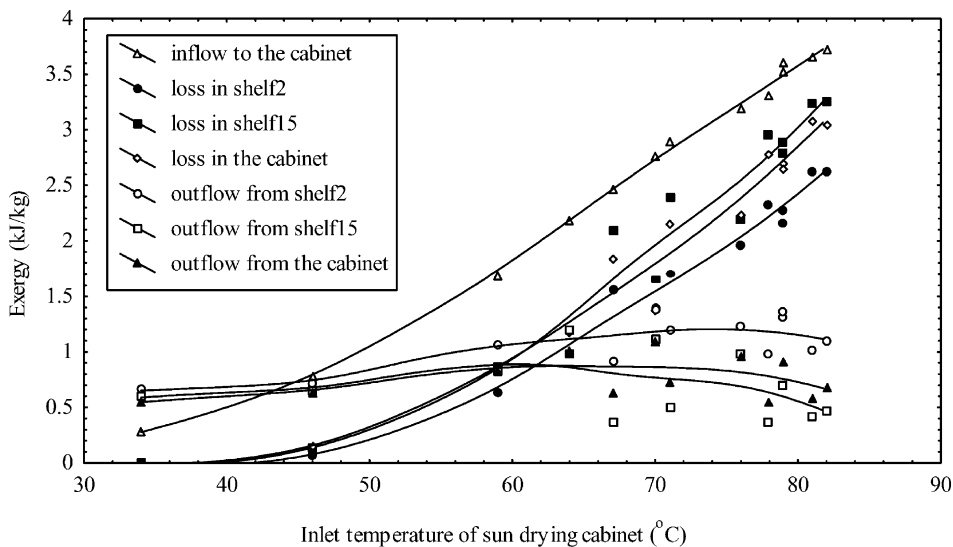


Fig. 8. Variations of exergy as a function of inlet temperature of solar drying cabinet.

useful energy gained from the solar air collectors was sufficient to dry the shelled and unshelled pistachios.

Fig. 6 displays the variation of the energy utilization on the left ordinate and the weight loss on the right as a function of drying time. The values of the energy utilization in the 2nd and 15th shelves were, respectively, calculated using Eqs. (16) and (17). The weight of shelled pistachio samples in the 2nd shelf decreased from 100 to 75.95 g in the ranges of 0–637 J s⁻¹ of the energy

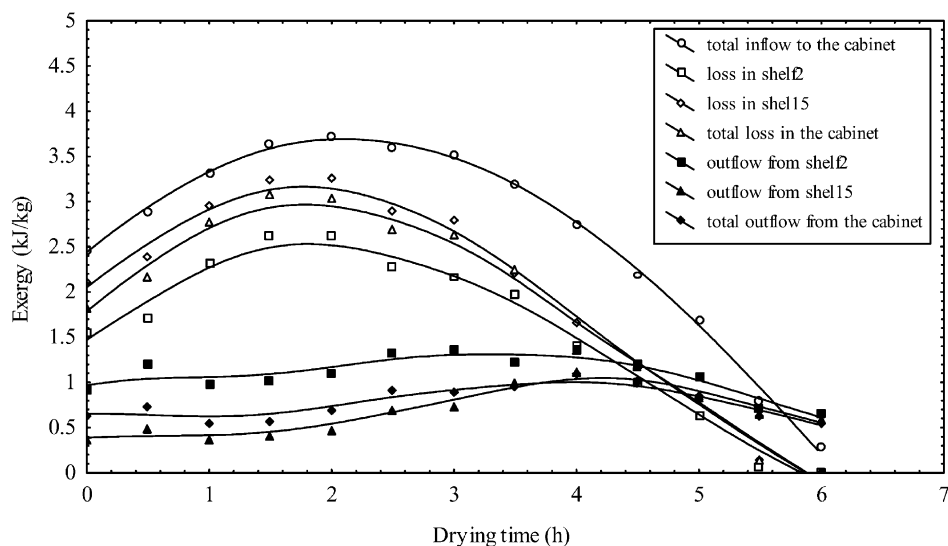


Fig. 9. Variations of exergy with drying time.

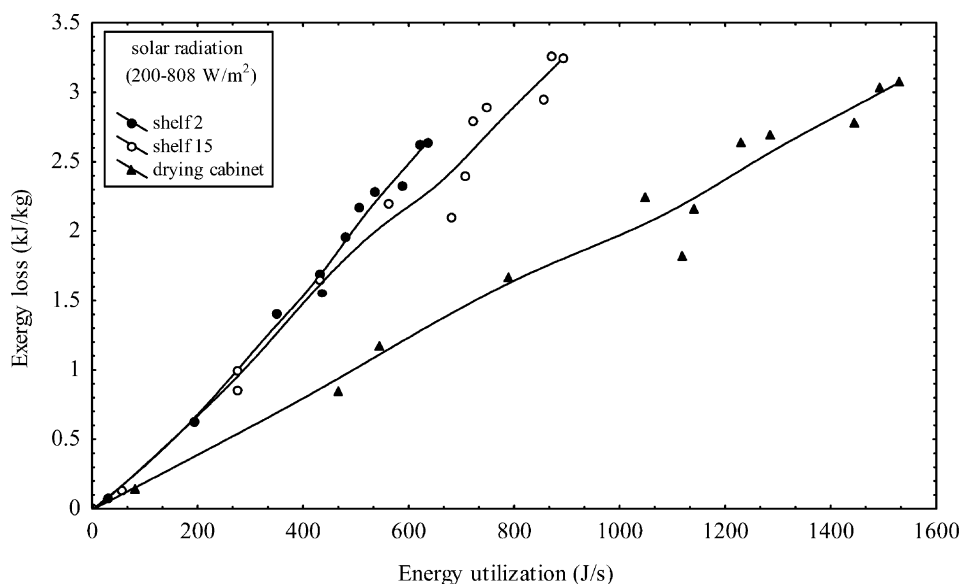


Fig. 10. Variations of exergy loss with energy utilization.

utilization. However, the unshelled pistachios in the 15th shelf reduced from 100 to 74.35 g in the ranges of 0–891 J s⁻¹ in 6 h. It was realized that unshelled pistachios consumed more energy than the shelled pistachios.

Fig. 7 exhibits the variation of the EUR as a function of drying time and Table 1 presents the results of the energy analysis of this process. EUR, calculated with Eqs. (19)–(21), was defined

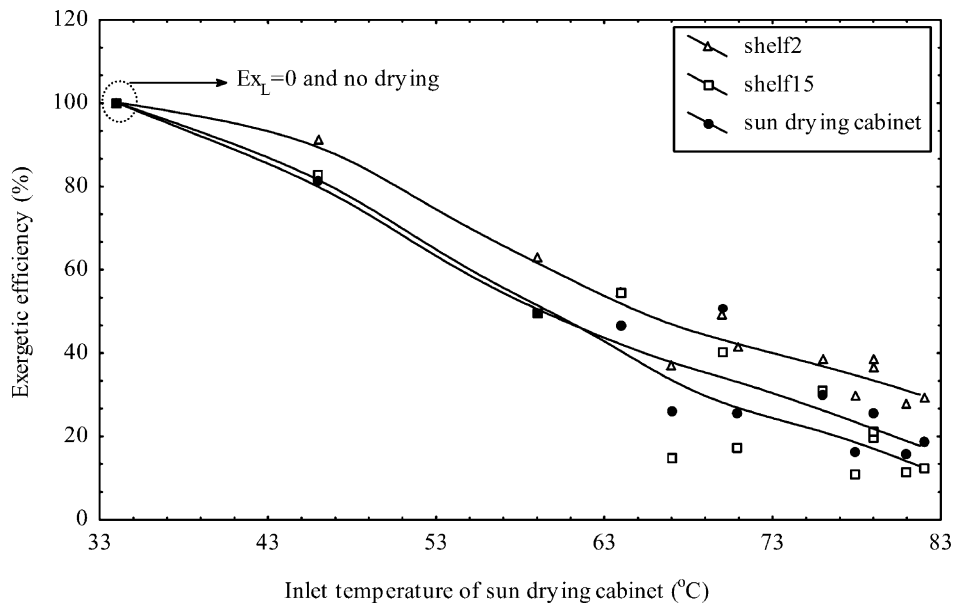


Fig. 11. Variations of exergetic efficiency as a function of inlet temperature of solar drying cabinet.

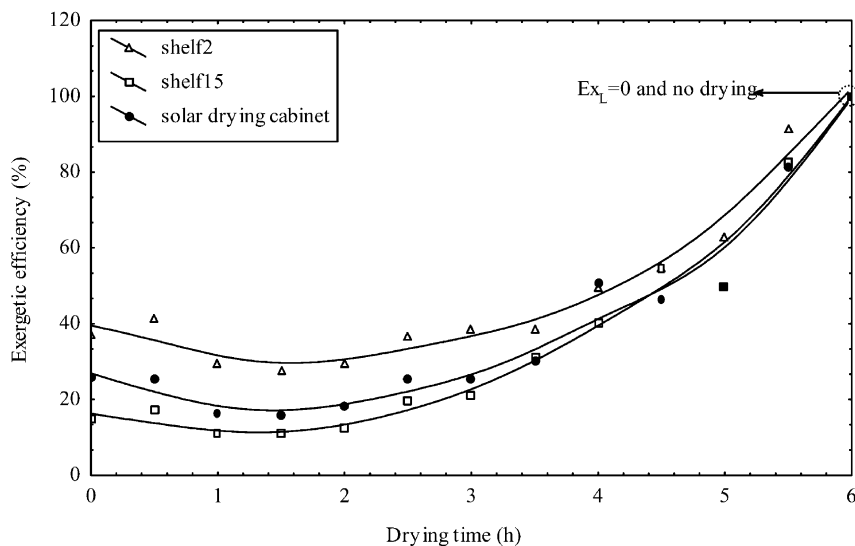


Fig. 12. Variation of exergetic efficiency as a function of drying time.

as the ratio of the energy utilization to the useful energy gained from the solar air collectors. It was noticed that EUR varied between 0 and 24.9% in the 2nd shelf, 0 and 34.8% in the 15th shelf, and 0 and 59.7% in the solar drying cabinet. Consequently, it was noticed that EUR of the 15th shelf was higher than that of the 2nd shelf. This resulted from the structure and the moisture content of the unshelled pistachios. Thus, it can be said that EUR is based on the structure and

Table 1
The results of energy analysis

Parameter	t (h)	T_{∞} (°C)	I (J s ⁻¹ m ⁻²)	E_{sac} (J s ⁻¹)	E_{shelf2} (J s ⁻¹)	E_{shelf15} (J s ⁻¹)
Experiment 1	0.00	27.00	660.50	2137.00	436.00	682.00
Experiment 2	0.50	27.50	725.00	2306.00	434.00	706.00
Experiment 3	1.00	31.00	771.00	2523.00	588.00	855.00
Experiment 4	1.50	31.50	799.00	2557.00	637.00	891.00
Experiment 5	2.00	32.00	808.00	2664.00	621.00	872.00
Experiment 6	2.50	30.00	799.00	2624.00	536.00	750.00
Experiment 7	3.00	30.50	789.00	2507.00	508.00	722.00
Experiment 8	3.50	30.00	753.00	2452.00	483.00	564.00
Experiment 9	4.00	27.50	697.00	2365.00	353.00	435.00
Experiment 10	4.50	26.50	614.00	2121.00	273.00	273.00
Experiment 11	5.00	26.20	531.00	1862.00	192.00	273.00
Experiment 12	5.50	24.00	356.00	1359.00	28.00	55.00
Experiment 13	6.00	21.00	200.00	977.00	0.00	0.00

Table 2
The results of the exergy analysis

Parameter	t (h)	T_{∞} (°C)	Ex_{di} (kJ kg ⁻¹)	Ex_{shelf2o} (kJ kg ⁻¹)	Ex_{shelf15o} (kJ kg ⁻¹)	Ex_{do} (kJ kg ⁻¹)	Ex_{dloss} (kJ kg ⁻¹)
Experiment 1	0.00	27.00	2.46	0.916	0.36	0.63	1.83
Experiment 2	0.50	27.50	2.89	1.192	0.49	0.73	2.16
Experiment 3	1.00	31.00	3.31	0.980	0.36	0.53	2.78
Experiment 4	1.50	31.50	3.65	1.017	0.41	0.57	3.08
Experiment 5	2.00	32.00	3.72	1.09	0.46	0.68	3.04
Experiment 6	2.50	30.00	3.60	1.31	0.70	0.91	2.69
Experiment 7	3.00	30.50	3.52	1.35	0.71	0.88	2.64
Experiment 8	3.50	30.00	3.19	1.23	0.98	0.95	2.24
Experiment 9	4.00	27.50	2.76	1.37	1.11	1.09	1.67
Experiment 10	4.50	26.50	2.18	1.20	1.20	1.01	1.17
Experiment 11	5.00	26.20	1.69	1.06	0.83	0.84	0.85
Experiment 12	5.50	24.00	0.78	0.71	0.65	0.63	0.15
Experiment 13	6.00	21.00	0.28	0.65	0.59	0.55	0.00

the moisture content of the dried products and could be assumed as an important parameter to analyze the energy utilization in drying processes.

Fig. 8 manifests the variation of exergy as a function of the inlet temperature of the solar drying cabinet. The exergy inflow rates were calculated using Eq. (25) depending on the ambient and inlet temperatures. The exergy inflow to the solar drying cabinet varied between 0.281 and 3.718 kJ kg⁻¹. However, the exergy outflows were added up with Eqs. (26)–(28). The values obtained were between 654 and 1.366 kJ kg⁻¹ for the 2nd shelf, 0.365 and 1.196 kJ kg⁻¹ for the 15th shelf, and 0.549 and 1.093 kJ kg⁻¹ for the cabinet. It was observed that the exergy inflow to the solar drying cabinet went up almost linearly with the increase of its inlet temperatures.

The exergy outflow from the 2nd shelf increased slowly until 70 °C and decreased slightly after that value while the exergy outflow from the 15th shelf went up to 64 °C and then came down. Additionally, the exergy losses were between 0 and 2.636 kJ kg⁻¹ for the 2nd shelf, 0 and 3.259 kJ kg⁻¹ for the 15th shelf, and 0 and 3.081 kJ kg⁻¹ for the cabinet by using Eq. (24). It was noticed that the exergy losses from the 2nd shelf were lower than those from the 15th shelf. Accordingly, the highest exergy outflow and the most efficient utilization of exergy were noticed in case of the minimum exergy losses in the system.

Fig. 9 shows the variation of exergy with drying time and Table 2 presents the results of the exergy analysis. The exergy inflow and the exergy loss to and from the shelves and the solar drying cabinet increased in the first 2 h, and then went down. The increase and decrease of the exergy inflow resulted from the variations of daily solar radiation. Moreover, the exergy outflow went up partially in the first 4 h, and then decreased slowly. However, the variations of the exergy loss in both the shelves and the cabinet stemmed from those of the ambient and outlet temperatures. The maximum value of the exergy inflow to the system was obtained as 3.718 kJ kg⁻¹. Thus, it can be inferred that it is necessary to show the variations of exergy with drying time in order to determine when and where the maximum and minimum values of the exergy losses took place during the solar drying process.

Fig. 10 shows the variation of the exergy loss with the energy utilization in both the shelves and the solar drying cabinet. Based on the amounts of the energy utilization, the exergy losses of the 2nd shelf varied between 0.07 and 2.64 kJ kg⁻¹, while those of the 15th shelf altered between 0.13 and 3.24 kJ kg⁻¹. Moreover, they increased linearly with the rise of the energy utilization in the cabinet. Accordingly, the exergy losses went up with the increase of the energy utilization in both the shelves and cabinet. Hence, it was noticed that the most exergy losses took place during the solar drying of unshelled pistachios.

Fig. 11 presents the variation of the exergetic efficiency as a function of the inlet temperature of the solar drying cabinet. The exergetic efficiency was calculated by using Eq. (29) based on the inflow, outflow, and loss of exergy. The exergetic efficiencies of the shelves and the cabinet decreased with the increase of inlet temperatures because the exergy losses of the shelves went up. They were 27.84–100% for the 2nd shelf, 10.86–100% for the 15th shelf, and 15.65–100% for the cabinet. It was realized that the exergy losses were equal to zero at the point where the exergetic efficiency was estimated as 100% due to discontinuity of drying process in the system. However, the exergetic efficiency of the 2nd shelf was higher than that of the 15th shelf and the cabinet. Therefore, it is said that the useful energy gained from the solar air collectors was productively utilized for the solar drying of shelled pistachios. That is, the highest exergetic efficiency was obtained during the solar drying of these products.

Fig. 12 shows the variation of the exergetic efficiency as a function of drying time. The exergetic efficiencies of the shelves and the cabinet decreased in the first 1.5 h, and then increased almost parabolically with the increase of drying time.

5. Conclusion

Energy and exergy analyses of the solar drying process of the shelled and unshelled pistachios were accomplished in this study. For these purposes, the products, supplied from Gaziantep, Tur-

key, were utilized. Considering the results of these analyses, the following conclusions may be drawn.

- The shelled and unshelled pistachio samples were sufficiently dried in the ranges between 40 and 60 °C, 200 and 808 W m⁻² of the solar radiation at 1.23 m s⁻¹ of drying air velocity in 6 h.
- The unshelled pistachio samples consumed more energy than the shelled pistachio samples between 200 and 808 W m⁻² of the solar radiation. The ratio of the energy utilization of the 15th shelf was higher than that of the 2nd shelf. This resulted from the structure and the moisture content of unshelled pistachio samples. The variation of EUR was based on the structure and the moisture content of the dried products. The EUR may be assumed as an important parameter to analyze the utilization of energy in drying processes.
- The most efficient use of exergy was achieved where and when exergy losses were minimum. The maximum value of the exergy inflow to the system was obtained as 3.718 kJ kg⁻¹. However, the exergy losses went up with the increase of the energy utilization in both the shelves and the solar drying cabinet. Although the most exergy losses took place during the solar drying of unshelled pistachios, the highest exergetic efficiency was obtained during the solar drying of shelled pistachios.
- The exergy losses were equal to zero at the point where the exergetic efficiency was estimated as 100% because drying process discontinued in the system.

Consequently, it is suggested that the order, structure, and moisture content of the products should be taken into consideration in order to decrease the energy utilization and the exergy losses.

Acknowledgements

The authors thank University of Nigde and Karadeniz Technical University for financial and technical supports.

References

- [1] Dutta K, Nema VK, Bhardwaj RK. Drying behavior of spherical grains. *Int J Heat Transfer* 1988;31:855–61.
- [2] Tiris C, Tiris M, Dincer I. Energy efficiency of a solar drying system. *Int J Energy Res* 1996;20:767–70.
- [3] Bejan A. Entropy generation through heat and fluid flow. New York: Wiley, 1982.
- [4] Bejan A. Advanced engineering thermodynamics. New York: Wiley, 1988.
- [5] Szargut J, Morris DR, Steward FR. Exergy analysis of thermal, chemical, and metallurgical processes. New York: Hemisphere, 1988.
- [6] Midilli A. Determination of pistachio drying behavior and conditions in a solar drying system. *Int J Energy Res* 2001;25(8):715–25.
- [7] Cengel YA, Boles MA. Thermodynamics: an engineering approach. New York: McGraw-Hill, 1994.
- [8] Ahern JE. The exergy method of energy systems analysis. New York: Wiley, 1980.
- [9] Verkhivker GP, Kosoy BV. On the exergy analysis of power plants. *Energy Convers Manage* 2001;42:2053–9.